LIMNOLOGY and OCEANOGRAPHY

ASLO

Limnol. Oceanogr. 9999, 2020, 1–13
© 2020 The Authors. *Limnology and Oceanography* published by Wiley Periodicals LLC. on behalf of Association for the Sciences of Limnology and Oceanography.
doi: 10.1002/lno.11557

Photosynthesis-driven methane production in oxic lake water as an important contributor to methane emission

Marco Günthel,[1*] **Isabell Klawonn**,[2] **Jason Woodhouse**,[2] **Mina Bižić**,[2] **Danny Ionescu**,[2] **Lars Ganzert**,[2] **Steffen Kümmel**,[3] **Ivonne Nijenhuis**,[3] **Luca Zoccarato**,[2] **Hans-Peter Grossart**,[2,4*] **Kam W. Tang**[1*]

[1]Department of Biosciences, Swansea University, Swansea, United Kingdom
[2]Department of Experimental Limnology, Leibniz Institute of Freshwater Ecology and Inland Fisheries, Stechlin, Germany
[3]Department for Isotope Biogeochemistry, Helmholtz Centre for Environmental Research-UFZ, Leipzig, Germany
[4]Institute of Biochemistry and Biology, Potsdam University, Potsdam, Germany

Abstract

Recent discovery of methane (CH_4) production in oxic waters challenges the conventional understanding of strict anoxic requirement for biological CH_4 production. High-resolution field measurements in Lake Stechlin, as well as incubation experiments, suggested that oxic-water CH_4 production occurred throughout much of the water column and was associated with phytoplankton especially diatoms, cyanobacteria, green algae, and cryptophytes. In situ concentrations and $\delta^{13}C$ values of CH_4 in oxic water were negatively correlated with soluble reactive phosphorus concentrations. Using ^{13}C-labeling techniques, we showed that bicarbonate was converted to CH_4, and the production exceeded oxidation at day, but was comparable at night. These experimental data, along with complementary field observations, indicate a clear link between photosynthesis and the CH_4 production-consumption balance in phosphorus-limited epilimnic waters. Comparison between surface CH_4 emission data and experimental CH_4 production rates suggested that the oxic CH_4 source significantly contributed to surface emission in Lake Stechlin. These findings call for re-examination of the aquatic CH_4 cycle and climate predictions.

The widely reported "methane paradox," that is, oversaturation of dissolved methane (CH_4) in oxic sea and lake waters (Tang et al. 2016), contradicts the conventional understanding that biological CH_4 production occurs exclusively under anoxic conditions (Thauer 1998; Ferry and Kastead 2007). Research in recent years has shown that active CH_4 production occurs in oxic sea (Karl et al. 2008; Damm et al. 2010) and lake waters (Grossart et al. 2011; Bogard et al. 2014; Tang et al. 2014). Globally, freshwaters account for about 122 ± 60 Tg yr^{-1} or about 20% of CH_4 emission to air (Saunois et al. 2016) and their contribution is expected to increase in future climate change scenarios (Dean et al. 2018). It is therefore necessary to understand the environmental dynamics of this oxic-water CH_4 source and its potential contribution to CH_4 emission to the atmosphere.

We investigated oxic-water CH_4 production in Lake Stechlin (Northeast Germany), an oligo-mesotrophic glacial lake in the temperate region that has been intensively monitored for decades (Casper 1985). Biological productivity in Lake Stechlin is phosphorus-limited (Casper 1985). Accordingly, the ratio of total nitrogen to total phosphorus in the epilimnion was (mean ± SD) 36 ± 9 during the study period in 2016 (March–July; $n = 15$) (Supporting Information Fig. S1), much higher than what is considered to indicate phosphorus limitation (i.e., a ratio of > 15 to > 22; Guildford et al. 2000; Abell et al. 2010). Recurring seasonal development of CH_4 oversaturation in the oxic midwater column has been observed in this lake, and previous studies have shown in situ oxic CH_4 production irrespective of CH_4 input from the sediment or lateral transport from the shore (Grossart et al. 2011; Tang et al. 2014). Despite skepticism (Fernandez et al. 2016; Peeters et al. 2019), mounting evidence for oxic-lake water CH_4 production suggests that this is a widespread

*Correspondence: hgrossart@igb-berlin.de (H.-P.G.); marcoguenthel@gmail.com (M.G.); k.w.tang@swansea.ac.uk (K.W.T.)

This is an open access article under the terms of the Creative Commons Attribution License, which permits use, distribution and reproduction in any medium, provided the original work is properly cited.

Additional Supporting Information may be found in the online version of this article.

Current affiliation of Lars Ganzert: Geomicrobiology Department, Helmholtz-Centre Potsdam GFZ, 14473 Potsdam, Germany

Author Contribution Statement: M.G., H.-P.G., and K.W.T. conceived the study. M.G., I.K., J.W., D.I., L.G., L.Z., and M.B. collected the field data. M.G., I.K., J.W., M.B., S.K., and I.N. collected the lab data. M.G. analyzed the data with input from coauthors. M.G. and K.W.T. wrote the manuscript with input from coauthors.

phenomenon in lakes (Grossart et al. 2011; Bogard et al. 2014; Tang et al. 2014; Donis et al. 2017; DelSontro et al. 2018; Günthel et al. 2019; Khatun et al. 2019). Currently, there are two proposed pathways for oxic-lake water CH_4 production: (1) Methane as a by-product of methylphosphonate (MPN) decomposition, which is an alternative way of phosphorus acquisition when inorganic phosphorus is limited (Carini et al. 2014; Yao et al. 2016; Wang et al. 2017); and (2) a pathway independent of MPN demethylation which is thought to be based on a Coenzyme-M homologue (Tang et al. 2016). Several studies have demonstrated the involvement of photoautotrophs in CH_4 formation in oxic water, both in the field (Grossart et al. 2011; Bogard et al. 2014; Hartmann et al. 2020) and in the laboratory (Lenhart et al. 2016; Klintzsch et al. 2019; Bizic et al. 2020; Hartmann et al. 2020). The association of oxic CH_4 production to MPN degradation and autotrophic organisms suggests that phosphorus and light might be important factors driving oxic CH_4 production.

We conducted a comprehensive study of the CH_4 dynamics in the oxic water of Lake Stechlin in order to address these questions: Which environmental factors promote oxic CH_4 production? How is oxic CH_4 production connected to phytoplankton? What is the contribution of this production to water-to-air CH_4 flux? To investigate the environmental parameters that promote oxic CH_4 production, we statistically analyzed the temporal and spatial CH_4 distributions and its isotopic signatures and different biotic and abiotic factors in the lake on seasonal, weekly, and diurnal time scales. Field observations were complemented by incubation experiments manipulating light and phosphorus availability. To test for the involvement of phytoplankton, we further analyzed in situ CH_4 concentration together with chlorophyll and taxon-specific pigment fluorescence data. Additionally, we conducted incubation experiments to measure depth-specific and size-specific CH_4 production rates, as well as incubation experiments with pure diatom culture. Using ^{13}C-labelling techniques, we showed that bicarbonate was converted to CH_4 in lake water, thereby establishing a direct link between photoautotrophic carbon fixation and oxic CH_4 production. The ^{13}C-label experiment was designed to quantify CH_4 production and consumption simultaneously throughout the diurnal cycle providing information about the effect of light on the CH_4 production-consumption balance. Last, the contribution of oxic CH_4 production to the water-to-air CH_4 flux was examined by comparing oxic production rates from incubation experiments with CH_4 emission rates to the atmosphere.

Materials and methods

Field measurements

Lake characteristics and sampling sites

Lake Stechlin is a dimictic meso-to-oligotrophic lake in Northeastern Germany. The lake has three basins with a combined surface area of 4.25 km^2 (volume ca. 0.09 km^3), a shoreline of 16.1 km and a catchment area of about 12.4 km^2 (26 km^2 subsurface catchment area). With 69.5 m maximum depth and 22.8 m mean depth, it is one of Germany's deepest lakes. More details can be accessed online via the monitoring station of the Leibniz-Institute of Freshwater Ecology and Inland Fisheries (https://www.igb-berlin.de/en/monitoring/stechlin) or the World Lake Database hosted by the International Lake Environment Committee (http://wldb.ilec.or.jp/Details/Lake/EUR-31).

Two locations in Lake Stechlin were sampled: (1) the northeast basin (69.5 m deep site; 53°09′20.2N 13°01′51.5E) and (2) the south basin (20.5 m deep site; 53°08′36.6″N 13°01′43.0″E). Data obtained for the northeast basin include environmental parameters (YSI probe data, partial BBE probe data, nutrients), CH_4 concentration profiles (0–20 m depth; March–July 2016), carbon isotope signatures of water column CH_4, and CH_4 surface emission rates. Data for the south basin sampling site include environmental parameters (YSI probe data, complete BBE probe data) and CH_4 concentration profiles (0–20 m depth; April–July 2016). Weather data were provided by the German Environment Agency (Neuglobsow weather station located directly next to the lake). Water samples collected for incubation experiments were collected in the south basin.

Environmental parameters

A YSI sonde Model 6600V2 was used to record temperature, dissolved oxygen, photosynthetically active radiation (PAR), and chlorophyll fluorescence. Concentrations of taxon-specific phytoplankton pigments were measured by a BBE Moldaenke Fluoroprobe. Parameter profiles were taken weekly during March–July 2016 at the deepest point (at 0, 2, 4, 6, 7, 8, 9, 10, 12, 14, 16, 18, and 20 m depth; YSI) and continuously every hour in the southern basin (0.5–20 m depth in 0.5 m intervals; YSI and BBE).

Nutrient concentrations were measured photometrically using a Foss Analytical FIAstar 5000 Analyzer with DDW detector and common standards: total phosphate (AN 5241, ISO 15681-1), soluble reactive phosphate (AN 5240, ISO 15681-1), total nitrogen (AN 5202D, DIN EN ISO 13395, ISO 11905), and NH_4-nitrogen (AN 5220, ISO 11732). Nutrient data were obtained weekly (May–July 2016) at 4, 7, 8, 10, and 12 m depth (deepest point).

Methane concentrations

Water was transferred from a Limnos Water Sampler to 50 mL serum bottles (clear borosilicate glass, ≥ 88% transmission of PAR spectrum), which were flushed three times then crimp-closed (PTFE-butyl septa, aluminum caps) without gas bubbles. Dissolved CH_4 was extracted using head space (Helium) displacement method and measured by a Shimadzu 14A GC/FID (35°C Permabond FFAP column on N_2, split-less injection, and detection at 140°C). Headspace CH_4 was converted to dissolved CH_4 concentrations based on Henry's Law and standard conditions. Seasonal CH_4 data were obtained in a 1-week interval; diurnal CH_4 data were collected

in 6-h intervals (only the last data point delayed by 1 h) from 8th July 2016 at 14:00 h local time until 11th July 2016 at 15:00 h (14:00 + n*6 h; 13 profiles). The standard deviations of measurements (averaged over depths) were ± 0.004 (northeast basin, triplicates) and ± 0.009 (south basin, duplicates) for the seasonal data, and ± 0.016 μmol L^{-1} (south basin, duplicates) for the diurnal data.

Methane emission

Emitted CH_4 was captured by a 15-liter floating chamber that was submerged at the perimeter by 3 cm and had a tube (butyl septum) at the center for gas sampling. Over 1–2 h, nine gas samples of each 20 mL were withdrawn by syringe, transferred into 50 mL serum bottles (prefilled with NaCl-saturated distilled water; PTFE septa enclosed), and the CH_4 concentrations were measured with GC/FID as described earlier. The CH_4 surface flux was then derived from linear regression over time.

Carbon isotope signature of water column methane

Anoxic sediment methanogenesis produces CH_4 with $\delta^{13}C$ values typically less than −55‰ (Whiticar 1999; Conrad et al. 2007). Methane oxidation at the sediment-water interface and within the water column preferentially enriches the ^{13}C content in the CH_4 pool, leading to $\delta^{13}C$ values greater than −55‰ in the water column (i.e., Whiticar 1999; Tang et al. 2014). Accordingly, changing water column $\delta^{13}C$ signatures to more negative values are commonly attributed to CH_4 production whereas changes to more positive values are attributed to CH_4 oxidation (Donis et al. 2017; DelSontro et al. 2018). The discovery of oxic CH_4 production, however, requires re-evaluation of this assumption. We used the water column ^{13}C signatures of CH_4 to statistically analyze its relation to environmental parameters.

To analyze the carbon isotope signature of water column CH_4, 5 mL gas samples extracted from lake water at different depths were stored in 12 mL Exetainer (prefilled with NaCl-saturated distilled water) and analyzed with a GC/C-IRMS unit composed of Agilent 7890A GC, GC IsoLink, a ConFlo IV interface to a MAT 253 IRMS (Thermo Fisher) and a programmed temperature vaporizer (MMI G3510A/G3511A, Agilent Technologies) with glass liner (1 cm CarboSieve SIII 60/80 packing). Compressed sample injection was done at −90°C (for 5.20 min, ramp 600°C min^{-1} until 225°C). A MolSieve 5A column (50 m × 0.32 mm × 30 μm) running on 2 mL min^{-1} He (35°C for 10 min, ramp 20°C min^{-1} until 250°C, final hold for 5 min) enabled separation. Carbon isotope signatures (of CH_4) are expressed in conventional $\delta^{13}C$ notation (‰) relative to Vienna-PeeDee Belemnite and were correlated to field parameter together with CH_4 concentration.

Linear modeling

R-software (R v3.3.1, RStudio v1.0.153) (RStudio Team, 2016) was used to test for linear relationships between parameters using general linear models, which were set up for γ-distribution and log-link, without interaction term unless stated otherwise. Regression results shown in scatter plots are based on LM models. Supporting Information Table S1 summarizes the correlations.

Experimental setups

Size fractionation experiment

A substantial part of the phytoplankton community was larger than freshwater methanogenic Archaea (commonly < 20 μm; Lyu and Liu 2019), and included cyanobacteria, diatoms, and green algae (Supporting Information Fig. S2). In this experiment, we examined which size fraction was responsible for CH_4 production in the oxic water, considering the fractions < 20 μm, > 20 μm, and nonfractionated.

One liter of an integrated lake water sample (4–8 m depth), taken on 3rd July 2018, was filtered through a 20 μm net creating the < 20 μm size fractions. Afterward, the filter was inverted and > 20 μm particles were resuspended in 1 L of sterile-filtered (0.2 μm) lake water, creating the > 20 μm size fraction. Unfiltered lake water was used as control. Water samples were added to 50 mL serum bottles (clear borosilicate glass, ≥ 88% transmission of PAR spectrum), air-saturated by bubbling atmospheric air for 10 min through a 0.2 μm filter and crimp-closed. Two bottles per size fraction were incubated for 24 h under natural day light exposure in the laboratory. Methane concentration was measured by a GC/FID unit and net CH_4 production was calculated as changing CH_4 concentration divided by incubation time.

Depth-specific methane production

Lake water from different depths was sampled in duplicates on 13th June 2016 and incubated in serum bottles (clear borosilicate glass, ≥ 88% transmission of PAR spectrum) in the laboratory exposed to natural daylight (on a shaker; room temperature). The CH_4 concentration was measured by GC/FID on day 0, 14, and 21. The average CH_4 production was calculated as changing CH_4 concentration divided by incubation time for two periods: day 0–14 (using CH_4 concentrations recorded on day 0 and 14) and day 0–21 (using CH_4 concentrations recorded on day 0 and 21).

^{13}C labeling experiment

To investigate the role of phytoplankton in oxic CH_4 production, lake water samples were spiked with dissolved inorganic carbon (DIC) as ^{13}C-labeled bicarbonate. The conversion of DIC to CH_4 was then measured as the incorporation of the ^{13}C label into the CH_4 product pool (IRMS analysis). Additionally, to quantify the CH_4 production-consumption balance in oxic water at different time of day, CH_4 oxidation was measured simultaneously by measuring the conversion of ^{13}C-labeled CH_4 to DIC.

Lake water (from 7 m depth) was collected on 1st September 2016, transferred to 12-mL Exetainer (clear soda lime glass, ≥ 91% transmission of PAR spectrum). To measure CH_4 production, three treatment groups were set up: (1) no $DI^{13}C$ addition, (2) addition of $DI^{13}C$, and (3) addition of $DI^{13}C$ and 1.4 mmol L^{-1} methyl fluoride (inhibitor of CH_4 oxidation; Chan and Parkin 2000) for control. $DI^{13}C$ was added in the

form of ^{13}C-labeled $NaHCO_3$ to a final labeling percentage of 21%. To measure CH_4 oxidation, three additional treatment groups were set up: (4) no $^{13}CH_4$ addition, (5) addition of $^{13}CH_4$, and (6) addition of $^{13}CH_4$ and 1.4 mmol L^{-1} methyl fluoride for control. The $^{13}CH_4$ was added to a final labeling percentage of 92.5%. Each treatment group included exetainers for the following time points (t_n; triplicate measurements): 0.3, 6.5, 15.5, 20.3, and 25.5 h (only first and last time points for the controls). All exetainers were placed in the lake at the original sampling depth and exposed to the ambient conditions; incubation started simultaneously at 16:00 h on 1st September 2016 (local time). After incubation, the corresponding water samples (t_n) were retrieved from the lake and microbial activity was stopped by adding 100 μL $ZnCl_2$ (saturated solution) per exetainer. For each time point, the ^{13}C content in the product pool (CH_4 for production; DIC for oxidation) was measured: Concentrations and ^{13}C signatures of CH_4 and DIC were measured by UC Davis (https://stableisotopefacility.ucdavis.edu/index.html). By comparing the ^{13}C content in the product pool between time t_n and start time t_0, the ^{13}C excess was calculated, which indicates average production/oxidation rates throughout the incubation periods (relative to how much substrate was labeled with ^{13}C).

The dimension of CH_4 oxidation and CH_4 production (pmol L^{-1} h^{-1}) were calculated as follows:

$$\mathrm{CH_4\ Oxidation} = \frac{C_{\mathrm{DIC,total}} * {}^{13}\mathrm{C\,atom\%\,excess}}{t * \mathrm{CH_4\ substrate\ label}} \quad (1)$$

$$\mathrm{CH_4\ Production} = \frac{C_{\mathrm{CH4,total}} * {}^{13}\mathrm{C\,atom\%\,excess}}{t * \mathrm{DIC\,substrate\,label}} + |\mathrm{CH_4\ Oxidation}| \quad (2)$$

Here, $C_{\mathrm{DIC/CH_4,total}}$ refers to overall concentration of DIC or CH_4; ^{13}C atom% excess (%) is the enrichment of ^{13}C in the sample computed via Eq. 3. t is the incubation time ($t_n - t_0$), t_n is sampling time point, and t_0 is starting time point. The *substrate label* is the of labeled substrates to the overall DIC or CH_4 (0.21 or 0.925).

$$^{13}\mathrm{C\,atom\%excess} = {}^{13}\mathrm{C\,atom\%}(t_n) - {}^{13}\mathrm{C\,atom\%}(t_0) \quad (3)$$

^{13}C atom% is the percentage of ^{13}C in the sample, calculated from Eq. 4:

$$^{13}\mathrm{C\,atom\%} = \frac{100 * \mathrm{nat.}{}^{13}\mathrm{C\,ratio} * \frac{\delta^{13}C_{\mathrm{VPDB}}}{100+1}}{1 * {}^{13}\mathrm{C\,ratio} * \frac{\delta^{13}C_{\mathrm{VPDB}}}{100+1}} \quad (4)$$

where $\delta^{13}C_{VPDB}$ is the relative deviation of sample ^{13}C from Vienna-PeeDee Belemnite ^{13}C (‰) and nat.^{13}C ratio refers to the natural abundance of ^{13}C isotopes.

Phosphorus addition experiment

In this experiment, we tested whether the addition of inorganic phosphorus to the lake water would affect the CH_4 production-consumption balance. An integrated lake water sample (4–8 m depth) was taken on 29th June 2018, filtered through a 100 μm net, mixed carefully by shaking, then added to serum bottles (clear borosilicate glass, ≥ 88% transmission of PAR spectrum) without disturbing the ambient gas conditions and crimp-closed (Teflon coated septa). The water sample was either untreated or enriched with 2.1 nmol (per 50 mL) K_2HPO_4 daily, and was incubated in the laboratory under natural day light exposure or in the dark. Microbial activity was stopped after incubation by adding $ZnCl_2$ to a final concentration of 0.5%. δ^{13}C of CH_4 (GC/IRMS; 2–5 measurements), soluble reactive phosphorus (SRP; Foss Analytical FIAstar 5000 Analyzer, one bottle sacrificed per time point), and oxygen saturation (PreSense sensor, one bottle sacrificed per time point) were measured at the start, and after 5 and 10 d of incubation.

Pure culture experiment

We measured the CH_4 production by two diatom cultures: *Navicula* sp. (isolated from Lake Stechlin) and *Leptocylindrus danicus* (marine), using a membrane inlet mass spectrometer (MIMS) and following the procedure of Bizic et al. (2020). The MIMS device (Bay Instruments, MD, U.S.A.) consisted of a crossbeam ion source mass spectrometer (Pfeiffer Vacuum, Germany), HiCube 80 Eco turbo pumping station (Pfeiffer Vacuum, Germany), QMG 220 M1, PrismaPlus®, C-SEM, 1-100 amu, and an experimental chamber. The experimental chamber (3.5 mL) contained an inner chamber for the culture and an outer chamber connected to a water bath to stabilize the temperature. The cultures were continuously mixed be a magnetic stirrer, kept at constant temperature, and incubated for 3 or 4 d under the following light regime: 19:30–09:00 h no light, gradually increasing to 60, 120, 180, and 400 μmol photon m^{-2} s^{-1} (1.5 h hold) then gradually decreasing in reverse order. A peristaltic pump (Minipuls3, Gibson) circulated the diatom cultures (constant temperature) continuously through a capillary linked to Viton pump tubing (Kana et al. 2006) kept in a water bath to stabilize the temperature and back to the culture (semi-closed system: no liquid loss, only gas loss). Throughout the circulation, the culture passed a microbore silicone membrane (8 mm, Silastic®, DuPont) permeable only to gases. The surrounding vacuum removed dissolved gases from the culture medium and fed it to the mass spectrometer where corresponding m/z ratios were recorded. The MIMS setup was calibrated to measure mass/charge ratio (m/z) in MilliQ water and growth media at different temperatures. Further calibration was realized by making measurements on air-saturated MilliQ water at different salinities.

To start, 3.5 mL culture were transferred to the experimental chamber and the m/z ratios representative of CH_4 (15) and oxygen (32) were recorded in a 9 s interval relative to the m/z ratio of argon (m/z = 40). Concentrations of CH_4, oxygen, and argon were calculated using published solubilities (Powell 1972). Production rates of CH_4 were calculated by first smoothing the raw data (sgolay function of the R package signal; 20 min interval; signal developers) (Signal Developers 2013) and then applying the 1st derivate. The degassing rate resulting from gas

consumption by the MIMS unit was determined experimentally and added to the absolute values of the 1st derivative. Final CH_4 production rates are presented relative to dry weight of the diatom biomass. To determine the dry weight, 3.5 mL diatom culture aliquot was filtered through a GF/F filter (combusted and preweighed; Millipore); the filter cake was subsequently dried (105°C) for 48 h and weighed at room temperature.

Results

Environmental setting

Seasonal scale

Seasonal CH_4 and environmental data for the south basin are presented in Fig. 1a–d and Supporting Information Fig. S3. Preliminary measurements prior to the seasonal study showed low CH_4 concentrations in the upper 20 m in the northeast basin, on average 0.02 and 0.03 μmol L^{-1} in February and March, respectively. As the lake began to stratify, upper water CH_4 concentration increased along with water temperature, reaching up to 1.4 μmol L^{-1} in late June at the thermocline depth (Fig. 1a). Strong CH_4 accumulations were consistently found in waters with oversaturated dissolved oxygen (up to 167%; 17 mg L^{-1}). Methane concentrations at 0–20 m depth were positively correlated with temperature ($p < 0.001$), PAR ($p < 0.001$), and oxygen saturation (up to 167% saturation) ($p < 0.001$). The concurrent total phosphorus was < 20 μg L^{-1}, SRP < 8 μg L^{-1}, total nitrogen < 1 mg L^{-1}, and ammonium < 0.05 mg L^{-1}. Further positive correlations were found between CH_4

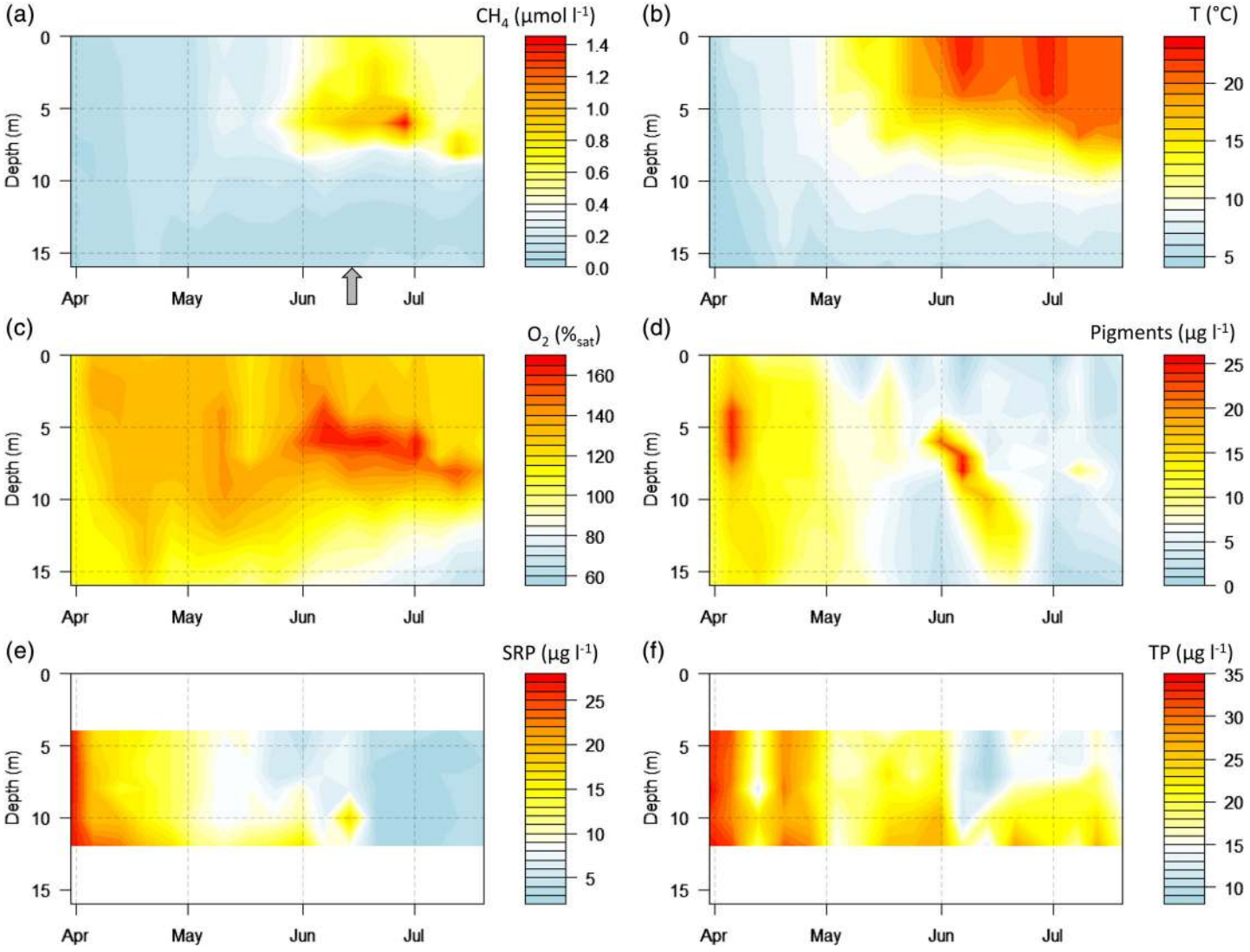

Fig. 1. Methane and environmental data—seasonal scale. (**a**) Methane concentration in μmol L^{-1}; (**b**) temperature in°C; (**c**) oxygen saturation in %; (**d**) combined pigment concentration of green algae, cyanobacteria, diatoms, and cryptophytes in μg L^{-1}; (**e**) SRP in μg L^{-1}; and (**f**) total phosphorus (TP) in μg L^{-1}. Methane (**a**) and probe data (**b**–**d**) were recorded in the south basin and nutrient data in the northeast basin (**e**, **f**). The arrow marks the time point of water sampling for investigating depth-specific methane production rates.

concentrations and pigment concentrations of cyanobacteria ($p < 0.001$), diatoms ($p < 0.001$, with temperature as interaction term), and cryptophytes ($p \leq 0.04$, with temperature as interaction term) at 0–20 m depth. Correlations are summarized in Supporting Information Table S1.

From the beginning of May to early June, the carbon isotope signature of water column CH_4 $\delta^{13}C$ scattered around −50‰ (± 2.5‰) (Fig. 2a). In mid-June, the $\delta^{13}C$ values increased to −45‰ to −37‰ (maximum at 7 m depth), then gradually decreased but remained greater than −50‰ in July. When plotted against SRP levels (Fig. 2b), both $\delta^{13}C$ values ($R^2 = 0.50$; $p < 0.001$) and concentrations of CH_4 ($R^2 = 0.21$; $p = 0.015$) showed negative correlations.

The water-to-air CH_4 flux increased by an order of magnitude between March and July (Fig. 3a), and generally followed the increasing amount of CH_4 in the upper 7 m (Fig. 1a), as well as increasing wind speed u_{10} (Supporting Information Fig. S4). Both CH_4 accumulation and emission showed a negative log-linear relationship with SRP concentrations in the upper 7 m (Fig. 3b). Supporting Information

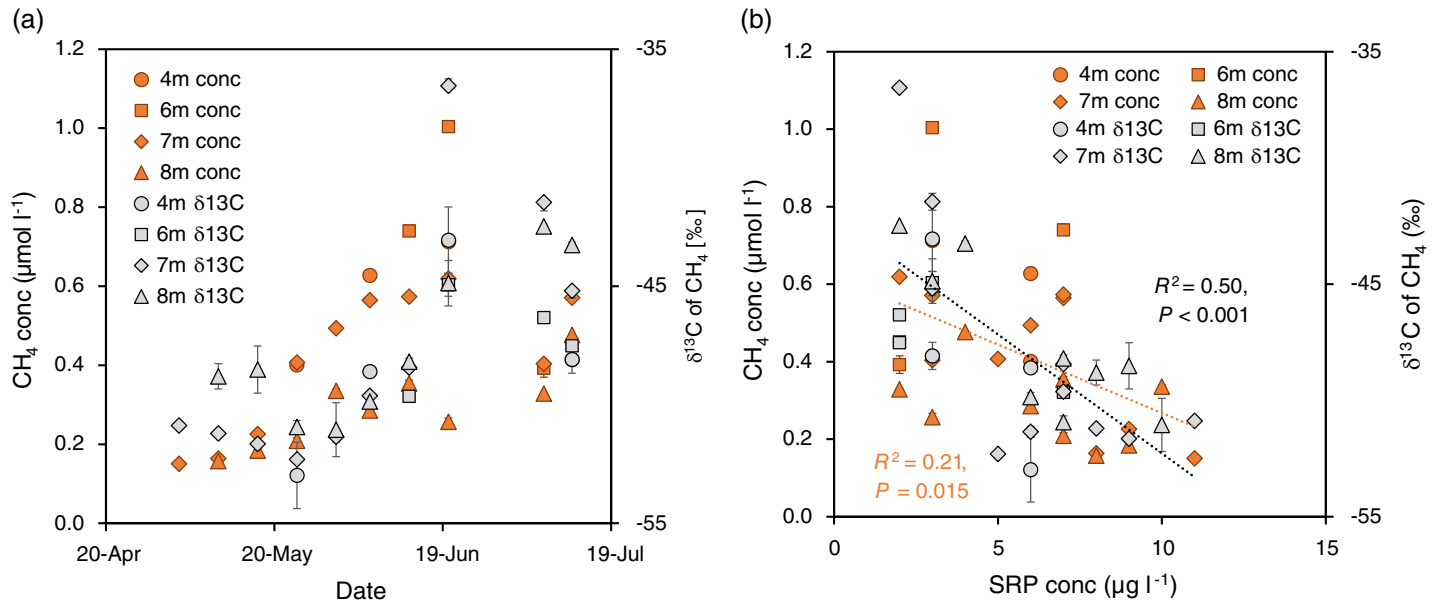

Fig. 2. Isotope characteristics of oxic methane accumulation. Methane concentrations and corresponding $\delta^{13}C$ values in relation to (**a**) time and (**b**) ambient SRP concentrations. CH_4 concentration ($R^2 = 0.21$, $p = 0.015$) and its ^{13}C signature ($R^2 = 0.50$, $p < 0.001$) correlated negatively with SRP concentration (CH_4 concentration/$\delta^{13}C$: mean ± SD of triplicate measurements).

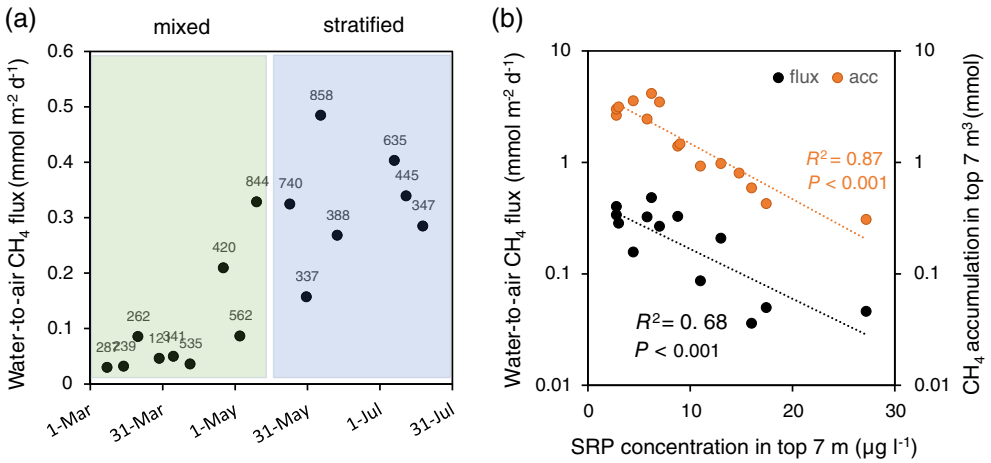

Fig. 3. Water-to-air CH_4 flux and environmental parameters. Panel (**a**) shows the seasonal increase in surface emission. Data points are labeled with radiation values (combined direct solar and reflected/scattered radiation) recorded at 21 m height (W m^{-2}). (**b**) Both surface emission ($R^2 = 0.68$, $p < 0.001$) and CH_4 accumulation in the upper 7 m ($R^2 = 0.87$, $p < 0.001$) significantly increased with decreasing SRP concentration (upper 7 m) in a log-linear fashion. Note that y-axes in panel (**b**) are in log-scale.

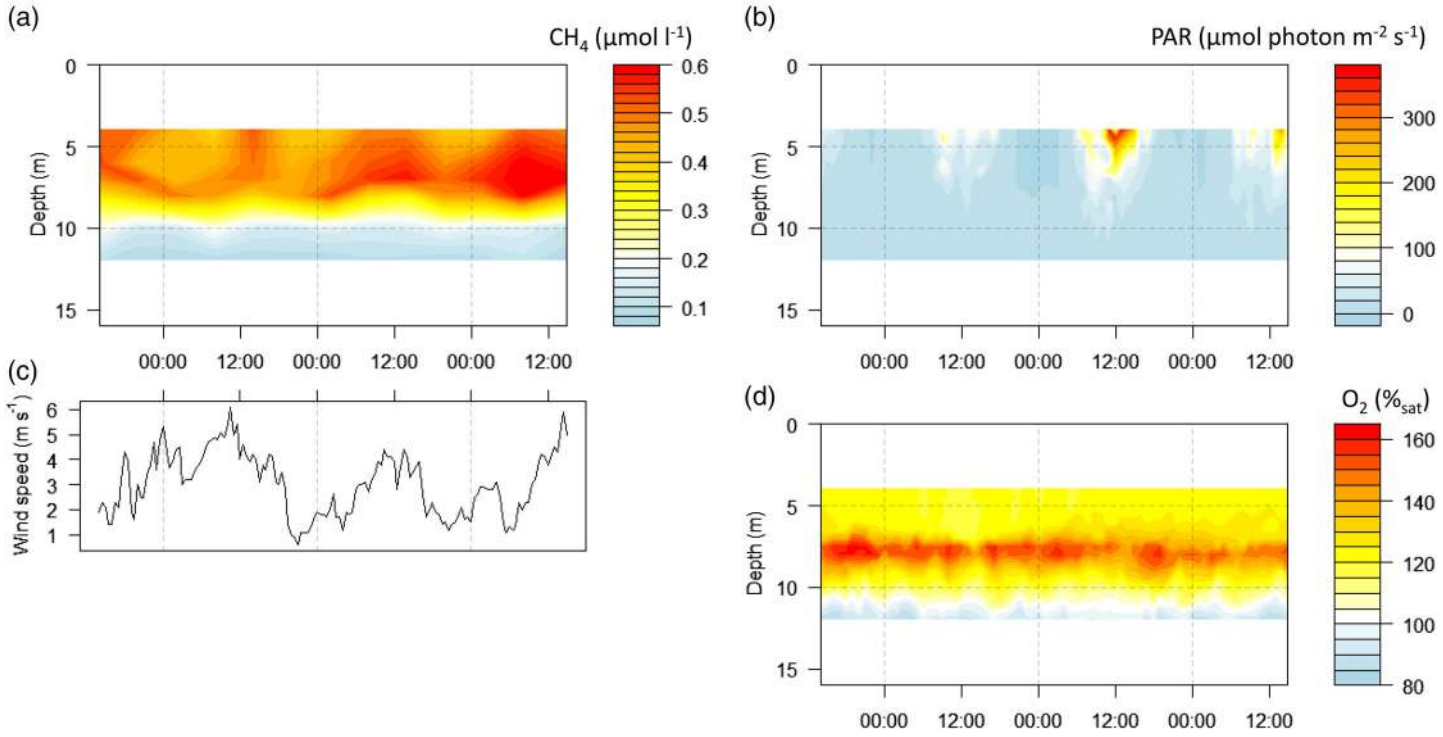

Fig. 4. Methane and environmental data—diurnal scale. (**a**) Methane concentration in μmol L^{-1}, (**b**) PAR in μmol photons m^{-2} s^{-1}, (**c**) wind speed u_{10} in m s^{-1} recorded at 10 m height, and (**d**) oxygen saturation in % throughout 8th–11th July 2016 in the south basin (24:00 h format; local time). The maximum diurnal CH_4 concentration recorded was 0.9 μmol L^{-1} during the last day of measurement at 08:00 h at 7 m depth, but the contour scale of panel (**a**) was limited to 0.6 μmol L^{-1} to provide better resolution of the diurnal pattern.

Table S2 summarizes the seasonal surface flux data and related environmental data.

Diurnal scale

Diurnal measurements revealed a rise-and-fall cycle of CH_4 in the water column (Fig. 4a–d; Supporting Information Fig. S5). During daylight at about 10:00–14:00 h local time, CH_4 concentrations increased to 0.6–0.9 μmol L^{-1}, whereas at night the concentrations dropped to about 0.4 μmol L^{-1}. The highest daily CH_4 accumulation coincided with the highest daily wind speeds around noon, showing variations in the CH_4 inventory throughout a diurnal cycle. Strong CH_4 accumulation consistently occurred at 7 m depth and at the 16°C isotherm, typically coinciding with high dissolved oxygen concentration (up to 16 mg L^{-1}; 162% saturation). The $\delta^{13}C$ values of CH_4 at 7 m varied between −43‰ and −47‰ over the day–night cycle (Supporting Information Fig. S6). Similar to the seasonal data, CH_4 showed a positive linear relationship with temperature ($p < 0.001$), PAR ($p = 0.003$), and oxygen saturation ($p < 0.001$) throughout the diurnal cycle. To account for diurnal differences in fluorescence response, we analyzed the daytime (05:00–21:30 h) and nighttime phytoplankton pigment data (21:30–05:00 h) separately, both of which gave positive relationships between CH_4 and chlorophyll (daytime: $p = 0.002$; nighttime: $p = 0.005$), green algae (daytime: $p < 0.001$; nighttime: $p < 0.001$), cyanobacteria (daytime: $p = 0.003$), and diatom pigment concentration (daytime: $p = 0.02$; nighttime: $p = 0.02$).

Methane production by phytoplankton

Size fraction experiment

We measured CH_4 production in the < 20 μm and > 20 μm size fractions of the lake water, as well as unfiltered lake water. The > 20 μm size fraction showed considerably higher net CH_4 production (mean ± SD) (19.2 ± 0.9 nmol L^{-1} d^{-1}) than the smaller fraction (4.3 ± 0.3 nmol L^{-1} d^{-1}) and unfiltered lake water (5.4 ± 0.3 nmol L^{-1} d^{-1}), suggesting that most of the CH_4 production was associated with large phytoplankton cells, colonies, and particles (Fig. 5a). Microscopic observations revealed that cyanobacteria, diatoms, and green algae were prevalent in the > 20 μm size fraction (Supporting Information Fig. S2). In comparison, CH_4 oxidation appeared to be primarily driven by cells smaller than 20 μm.

Depth-specific methane production

Water samples collected in the epilimnion, thermocline, and hypolimnion (0–20 m sampled; ca. 20.5 m deep site) all showed increasing CH_4 concentrations over time when incubated under natural daylight in the laboratory (Fig. 5b), and the highest production rates were found in waters collected

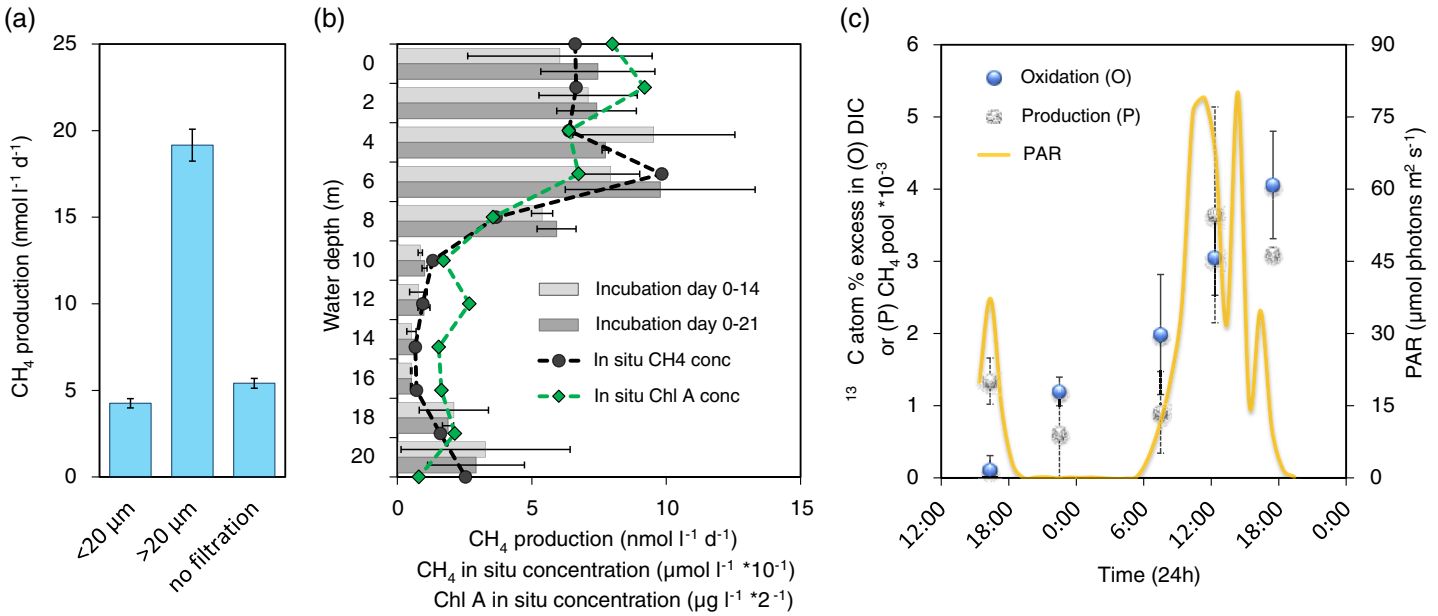

Fig. 5. Bottle incubation experiments. (**a**) Net CH_4 production rates of size-fractionated lake water vs. untreated lake water (mean ± SD, $n = 2$). (**b**) Depth-specific net CH_4 production rates (bars; mean ± SD, $n = 2$). The profile production rates mimic the profile of in situ CH_4 concentration (dotted symbols/line) and the profile of in situ Chl *a* concentration (green symbols/line). Note: for better illustration purpose, water samples taken from 7 and 9 m depth are not depicted (full data in Supporting Information Table S3). (**c**) CH_4 oxidation and CH_4 production as deduced from ^{13}C-label substrate turnover (oxidation: $^{13}CH_4$; production: $DI^{13}C$) (mean ± SD, $n = 3$). Photosynthetically active radiation at ambient depth is symbolized by PAR. The average increasing ^{13}C excess over time in the DIC pool (= oxidation) had a positive linear slope ($R^2 = 0.98$; $p < 0.002$) whereas the average ^{13}C excess in the CH_4 pool (= production) did not show a significant linear slope ($R^2 = 0.54$; $p = 0.16$).

from the epilimnion and thermocline depth. Methane production was significantly correlated with in situ CH_4 concentration (incubation day 0–14: $R^2 = 0.77$, $p < 0.001$; incubation day 0–21: $R^2 = 0.83$, $p < 0.001$) and chlorophyll *a* (Chl *a*) concentration in the corresponding depths (incubation day 0–14: $R^2 = 0.68$, $p < 0.001$; incubation day 0–21: $R^2 = 0.75$, $p < 0.001$) (Supporting Information Table S3). Thus, waters collected from depths with high in situ CH_4 concentration showed high CH_4 production, and vice versa.

^{13}C labeling experiment

In this experiment, CH_4 oxidation and CH_4 production were measured using ^{13}C-labeled substrates and recording the incorporation of ^{13}C into the respective product pools over time. Thermocline-depth water samples treated with $^{13}CH_4$ showed a linear increase in incorporation of ^{13}C into the DIC pool over time (Fig. 5c), whereas samples treated with methyl fluoride to inhibit CH_4 oxidation showed negligible change in $DI^{13}C$. The difference between the two treatments gave a CH_4 oxidation of 1.9 ± 0.3 pmol L^{-1} h^{-1} (Eq. 1). In the parallel treatment groups, the addition of $NaH^{13}CO_3$ resulted in incorporation of ^{13}C into the CH_4 pool (Fig. 5c). There was a small decrease in the $^{13}CH_4$ pool at night even with added methyl fluoride, suggesting incomplete inhibition of CH_4 oxidation, whereas ^{13}C incorporation into CH_4 during daytime exceeded the nighttime loss. Based on ^{13}C incorporation, the net change in CH_4 varied between −1.4 (night) and 7 pmol L^{-1} h^{-1} (day) throughout the diurnal cycle (Fig. 5c). Using Eq. 2 and applying the average oxidation rate from the $^{13}CH_4$ labeling experiment, the gross CH_4 production was estimated to be 0.5 (night) and 8.9 pmol L^{-1} h^{-1} (day). The results are summarized in Supporting Information Tables S4 and S5.

Phosphorus addition experiment

An integrated lake water sample was taken from 4 to 8 m depth during the stratified and phosphorus limited season (SRP ≤ 3 µg L^{-1}) (Supporting Information Fig. S7). This lake water was incubated in the laboratory under natural daylight exposure or in darkness, with or without the addition of K_2HPO_4. All treatment groups remained oxic throughout the experiment and $\delta^{13}C$ values varied among the treatment groups (Supporting Information Fig. S8 and Table S6). While the addition of phosphorus shifted $\delta^{13}C$ to more negative values in the light treatment, dark incubation resulted in more positive $\delta^{13}C$ values.

Pure culture experiment

Both the freshwater diatom *Navicula* sp. and the marine diatom *Leptocylindrus danicus* showed CH_4 production (Fig. 6). Highest CH_4 production rates were observed during the light periods, especially during highest light intensities. During dark phases production rates were low (both species) or undetectable (*Navicula* sp.). A decrease in CH_4 concentration could be the result of either decreased or no production coupled with degassing from the supersaturated, continuously

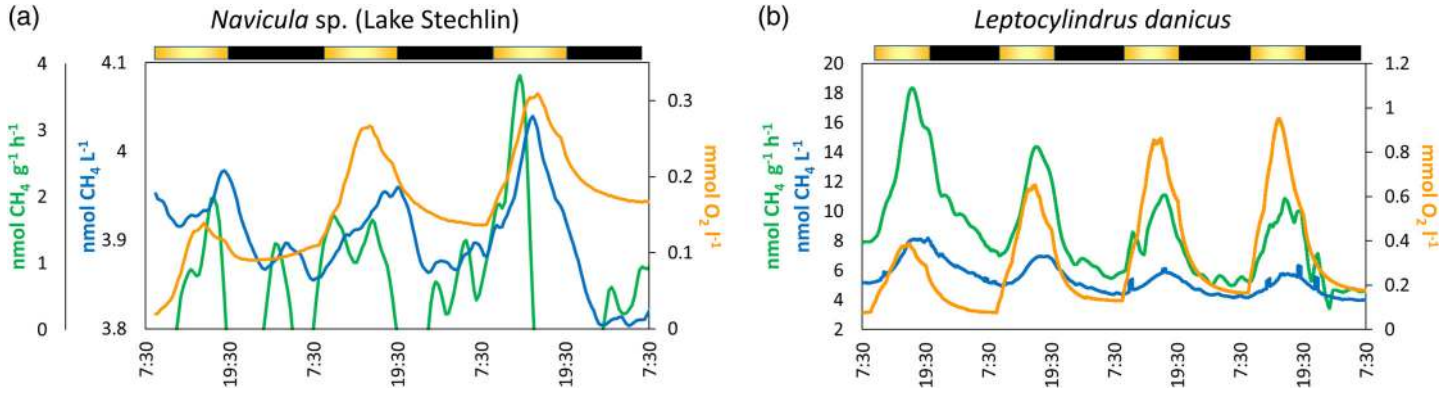

Fig. 6. Pure culture experiments. Membrane inlet mass spectrometry (MIMS) was deployed to record methane and oxygen throughout incubation of (**a**) the freshwater diatom *Navicula* sp. (isolated from Lake Stechlin), and (**b**) the marine diatom *Leptocylindrus danicus*. The blue line resembles methane concentration, the green line is methane production normalized to dry weight, and the yellow line is the oxygen concentration inside the experimental MIMS chamber. A Savitzky-Golay filter (20 min interval) was applied to remove outlier data points. The light regime for the experiments was as follows: dark (black bar) from 19:30 h to 09:00 h then light intensity was programmed to increase to 60, 120, 180, and 400 μmol photon m^{-2} s^{-1} with a hold time of 1.5 h at each intensity (yellow to white bar). After maximum light period, the intensity was programmed to decrease in reverse order with the same hold times until complete darkness again at 19:30 h.

mixing, semi-closed incubation chamber toward equilibrium with atmospheric CH_4 (2.5 nmol L^{-1} and 2.1 nmol L^{-1} for freshwater and seawater, respectively).

Discussion

Environmental setting

Methane accumulation in oxic surface waters of temperate lakes often coincides with seasonal stratification (Bastviken et al. 2008; Tang et al. 2016). In our study, CH_4 concentrations were up to 115 times higher in the summer months than in early spring, leading to a 29-fold increase in total CH_4 in the top 7 m of the strongly oxygenated water column (> 100 % saturation; > 10 mg L^{-1}) between late March and July.

While it is common to describe CH_4 dynamics based on either exclusively CH_4 concentration data (e.g., Juutinen et al. 2009; Li et al. 2018) or exclusively CH_4 isotope data (e.g., Cadieux et al. 2016; Lecher et al. 2017), by combining both data types we revealed a new aspect of CH_4 dynamics in the water column. For example, when considering CH_4 concentration alone, the increase in in situ mid-water CH_4 between March and July (Fig. 2a) can be interpreted as the result of a stronger or accumulating CH_4 input from sediments and littoral zone, which would be accompanied by a decrease in the corresponding $\delta^{13}C$ value indicative of anoxic CH_4 (Whiticar 1999). Conversely, when only considering CH_4 isotope data alone, the observed ^{13}C enrichment throughout June (Fig. 2a) can be interpreted as an increase in CH_4 oxidation activity, which should also lead to a decrease in the corresponding CH_4 concentration (Whiticar 1999). However, by combining both data sets we showed a concurrent increase in both CH_4 concentration (from ca. 0.3/0.6 to 1.0 μmol L^{-1}) and $\delta^{13}C$ signature (from ca. −52‰ to −37‰). Our observations allow the alternative explanation of an internal (oxic) CH_4 source with a $\delta^{13}C$ signature distinctively higher than that of the anoxic CH_4 sources. This explanation is supported by our bottle incubations showing active CH_4 production under oxic conditions, and a recent study modeling CH_4 carbon isotope changes in lake water (Hartmann et al. 2020).

Phosphorus deficiency has been shown to promote demethylation of MPNs with subsequent CH_4 release in both marine and freshwater environments (Carini et al. 2014; Repeta et al. 2016; Yao et al. 2016; Wang et al. 2017). Methyl groups cleaved from the C-1 compounds are converted to CH_4 by a reductase, potentially drawing the required reductive power via electron dumping from photosynthesis (Tang et al. 2014), especially under nutrient limitation (Hemschemeier and Happe 2011). This hypothesis is corroborated by our field and lab measurements together showing that oxic CH_4 production was connected to photosynthesis as well as low SRP concentrations. Nevertheless, it remains unclear whether the MPN pathway would result in CH_4 with $\delta^{13}C$ values greater than −40‰ (kinetic isotope effects strongly depend on elemental composition and molecule configuration; therefore, incubation experiments with enriched MPN pool as CH_4 precursor do not reflect the natural $\delta^{13}C$ response in the field).

Methane production by phytoplankton

Several lines of evidence point to the direct role of phytoplankton in oxic CH_4 production in our study. First, in situ CH_4 concentrations were positively correlated to PAR, phytoplankton pigment concentrations, and oxygen (over)saturation (as a by-product of photosynthesis). Second, our diurnal measurements showed a cyclical CH_4 pattern in the water

column that aligned with the light–dark periods. Third, highest CH_4 production was observed in the > 20 μm size fraction, which contained mostly cyanobacteria, diatoms, and green algae. Our light incubations using lake water amended with K_2HPO_4 resulted in a $\delta^{13}C$ shift toward more negative values, whereas dark incubation resulted in more positive values, together indicating that CH_4 production was triggered by light. The alternative explanation of light-inhibited CH_4 oxidation (Murase and Sugimoto 2005) is unlikely to be relevant because our ^{13}C-labeling experiment showed constant oxidation rates throughout the diurnal cycle (Fig. 4c). Further direct evidence was provided by incubation with $NaH^{13}CO_3$ resulting in a much higher incorporation of ^{13}C into CH_4 in daytime vs. nighttime, showing that photoautotrophic carbon fixation was involved in the process, as we hypothesized earlier (Tang et al. 2014). Among the major phytoplankton groups, cyanobacteria showed the strongest and most consistent positive correlation with CH_4 concentrations in situ, implicating their key role in oxic CH_4 production. Using cyanobacteria cultures and a MIMS, Bizic et al. (2020) showed that CH_4 production follows the light–dark cycle with a small time-lag. Here, we conducted similar MIMS measurements with cultures of the freshwater diatom *Navicula* sp. (isolated from Lake Stechlin) and the marine diatom *Leptocylindrus danicus* (Fig. 6). Both species showed CH_4 production aligning with light–dark incubation periods and more CH_4 was produced at higher light intensities. Combining ours and others' findings (Bizic et al. 2020; Hartmann et al. 2020), the results suggest that light-triggered CH_4 production may be common among phytoplankton. It is likely that the conversion of $NaH^{13}CO_3$ to CH_4 involves multiple steps, not all being light-dependent (decreased but active CH_4 production during dark phases: Bizic et al. 2020; Fig. 6). Nevertheless, the observations that oxic CH_4 production was linked to photosynthesis indicate that the oxic and anoxic methane sources will react differently to environmental perturbations.

In the marine environment, the cyanobacterium *Trichodesmium erythraeum* has been found to carry gene cassettes encoding the enzymes for the conversion of MPNs to CH_4 (Dyhrman et al. 2006; Beversdorf et al. 2010). Similar genes have been found in the freshwater cyanobacterium *Picocyanobacterium* (Kutovaya et al. 2013; Yao et al. 2016). However, in previous studies, enrichment of Lake Stechlin water with MPNs has produced conflicting results in stimulating CH_4 production (Grossart et al. 2011; Bizic-Ionescu et al. 2018). Another possible pathway involves nitrogenase enzymes, which are common among cyanobacteria (Bothe et al. 2010). Iron-only nitrogenases of wild-type proteobacteria have been shown to convert carbon dioxide, nitrogen gas and protons to CH_4 in a single enzymatic reaction, and the CH_4 yield increases with increasing light intensity (up to 30 μmol photons m^{-2} s^{-1}) (Zheng et al. 2018). Furthermore, this reaction has been found in an obligate aerobic bacterium, *Azotobacter vinelandii* (Zheng et al. 2018). However, the iron-only nitrogenase activity has never been demonstrated in CH_4 production by cyanobacteria. Diatoms are generally incapable of nitrogen-fixation; therefore, the observed CH_4 production (Fig. 6) indicates that the underlying mechanism does not necessarily require nitrogenase.

Implication for methane emission to the atmosphere

Measured net CH_4 production was comparable above and within the thermocline; loss of CH_4 to oxidation and diffusion within the epilimnion could result in a concentration gradient with the CH_4 maximum at the thermocline as observed. An earlier study did not detect more methane oxidizer in surface water compared to thermocline water (Grossart et al. 2011); therefore, it is more likely that the gradient was caused by diffusive loss of CH_4 across the water–air interface, which is corroborated by our surface flux measurements. To explain the observed average surface flux of 0.32 mmol m^{-2} d^{-1} during the stratified season (after 17th May), it would require an oxic production of 46 nmol L^{-1} d^{-1} in the upper 7 m. In our incubation experiment, water collected from the upper 7 m yielded about 8 nmol L^{-1} d^{-1} oxic CH_4 production. Our measurement represents only a snapshot of the system and does not fully capture the natural variability of CH_4 production. For example, Grossart et al. (2011) reported about seven times higher oxic CH_4 production rate in an earlier year based on bottle incubations. Günthel et al. (2019) and Hartmann et al. (2020), using mass balance analysis of CH_4 production and loss, arrived at oxic CH_4 production rates of up to > 200 nmol L^{-1} d^{-1}. Therefore, our oxic CH_4 production rates should be considered conservative, which potentially explained 18% of the observed average surface flux. Similarly, recent investigations in the mesotrophic Lake Hallwil, Switzerland found that about 63–90% of CH_4 emission could be attributed to oxic CH_4 production and accumulation in the upper mixed layer (Donis et al. 2017; Günthel et al. 2019). Light and phosphorus were found in our incubation experiments to be important factors for oxic CH_4 production, which is consistent with our field observations that the water-to-air CH_4 flux correlates with both parameters. Together, our observations suggest that oxic CH_4 production in the upper layer is an important contributor to CH_4 emission, but hitherto has not been acknowledged in global methane budgets and models (IPCC 2013).

Reconsidering the methane paradox

The methane paradox is rooted in the paradigm that biological CH_4 production occurs strictly under anoxic conditions and therefore, oxic-water CH_4 oversaturation is often exclusively attributed to physical transport from anoxic sources. However, reports of oxic CH_4 production by terrestrial flora and fauna have prompted questions of this paradigm (Keppler et al. 2006; Ghyczy et al. 2008; Lenhart et al. 2012; Althoff et al. 2014). Similarly, the mounting evidence in both marine and freshwater environments (Tang et al. 2016) and reference therein,

including this study, has demonstrated unequivocally that active biological CH_4 production occurs in oxic waters. Accordingly, the methane paradox can be explained, at least partially, by internal oxic production (Grossart et al. 2011; Tang et al. 2014; Günthel et al. 2019), with or without external inputs (Fernandez et al. 2016; DelSontro et al. 2018; Peeters et al. 2019).

Pure-culture experiments demonstrated the ability of oxic CH_4 production in diatoms (Hartmann et al. 2020; this study), cyanobacteria (Bizic et al. 2020), green algae, and cryptophytes (Hartmann et al. 2020). Additionally, our study showed the conversion of (^{13}C-labeled) bicarbonate to CH_4 demonstrating a direct link of oxic CH_4 production to photosynthesis, and our field data corroborate the involvement of diatoms, cyanobacteria, green algae, and cryptophytes. While the precise biochemical pathway(s) is subject to further investigation, these findings together indicate CH_4 production may be a common feature among diverse phytoplankton taxa. Phytoplankton are ubiquitous in illuminated aquatic environments and are globally on the rise (Hampton et al. 2008; Duan et al. 2009; Ho et al. 2019). It is therefore necessary to understand how these potential oxic methane producers react to environmental perturbation such as widespread eutrophication and global warming, and the corresponding effect on atmospheric CH_4 emission. Available data for Lake Stechlin (Günthel et al. 2019, Hartmann et al. 2020; this study), Lake Cromwell (Bogard et al. 2014) and Lake Hallwil (Donis et al. 2017, Günthel et al. 2019) show that oxic CH_4 production can account for 18–90% of the surface emission. Albeit limited, these findings warrant an urgent re-examination of the (aquatic) CH_4 cycle (Kirschke et al. 2013; Saunois et al. 2016) and climate change predictions (IPCC 2013) that are presently based on almost exclusively conventional anoxic CH_4 sources.

Data availability statement

Manuscript related data are available in tabular form in the Supporting Information (incubation experiments, flux data) and via GLEON data repositories upon acceptance (seasonal and diurnal field data) (http://gleon.org/).

References

Abell, J. M., D. Özkundakci, and D. P. Hamilton. 2010. Nitrogen and phosphorus limitation of phytoplankton growth in New Zealand lakes: Implications for eutrophication control. Ecosystems **13**: 966–977. doi:10.1007/s10021-010-9367-9

Althoff, F., K. Benzing, P. Comba, C. McRoberts, D. R. Boyd, S. Greiner, and F. Keppler. 2014. Abiotic methanogenesis from organosulphur compounds under ambient conditions. Nat. Commun. **5**: 4205. doi:10.1038/ncomms5205

Bastviken, D., J. J. Cole, M. L. Pace, and M. C. Van de Bogert. 2008. Fates of methane from different lake habitats: Connecting whole-lake budgets and CH_4 emissions. J. Geophys. Res. Biogeosci. **113**: 1–13. doi:10.1029/2007JG000608

Beversdorf, L. J., A. E. White, K. M. Björkman, R. M. Letelier, and D. M. Karl. 2010. Phosphonate metabolism by *Trichodesmium* IMS101 and the production of greenhouse gases. Limnol. Oceanogr. **55**: 1768–1778. doi:10.4319/lo.2010.55.4.1768

Bizic, M., and others. 2020. Aquatic and terrestrial cyanobacteria produce methane. Sci. Adv. **6**: eaax5343. doi:10.1126/sciadv.aax5343

Bizic-Ionescu, M., D. Ionescu, M. Günthel, K. W. Tang, and H.-P. Grossart. 2018. Oxic methane cycling: New evidence for methane formation in oxic lake water, p. 1–22. *In* J. M. Alfons and D. Sousa [eds.], Biogenesis of hydrocarbons. Springer.

Bogard, M., P. A. del Giorgio, L. Boutet, M. C. Garcia-Chaves, Y. T. Prairie, A. Merante, and A. M. Derry. 2014. Oxic water column methanogenesis as a major component of aquatic CH_4 fluxes. Nat. Commun. **5**: 5350. doi:10.1038/ncomms6350

Bothe, H., O. Schmitz, M. G. Yates, and W. E. Newton. 2010. Nitrogen fixation and hydrogen metabolism in cyanobacteria. Microbiol. Mol. Biol. Rev. **74**: 529–551. doi:10.1128/MMBR.00033-10

Cadieux, S. B., J. R. White, P. E. Sauer, Y. Peng, A. E. Goldman, and L. M. Pratt. 2016. Large fractionations of C and H isotopes related to methane oxidation in Arctic lakes. Geochim. Cosmochim Acta **187**: 141–155. doi:10.1016/j.gca.2016.05.004

Carini, P., A. E. White, E. O. Campbell, and S. J. Giovannoni. 2014. Methane production by phosphate-starved SAR11 chemoheterotrophic marine bacteria. Nat. Commun. **5**: 4346. doi:10.1038/ncomms5346

Casper, S. J. 1985. Lake Stechlin: A temperate oligotrophic lake. Dr W. Junk Publishers.

Chan, A. S. K., and T. B. Parkin. 2000. Evaluation of potential inhibitors of methanogenesis and methane oxidation in a landfill cover soil. Soil Biol. Biochem. **32**: 1581–1590. doi:10.1016/S0038-0717(00)00071-7

Conrad, R., O.-C. Chan, P. Claus, and P. Casper. 2007. Characterization of methanogenic Archaea and stable isotope fractionation during methane production in the profundal sediment of an oligotrophic lake (Lake Stechlin, Germany). Limnol. Oceanogr. **52**: 1393–1406. doi:10.4319/lo.2007.52.4.1393

Damm, E., E. Helmke, S. Thoms, U. Schauer, E. Nöthig, K. Bakker, and R. P. Kiene. 2010. Methane production in aerobic oligotrophic surface water in the central Arctic Ocean. Biogeosciences **7**: 1099–1108. doi:10.5194/bg-7-1099-2010

Dean, J. F., and others. 2018. Methane feedbacks to the global climate system in a warmer world. Rev. Geophys. **56**: 207–250. doi:10.1002/2017RG000559

DelSontro, T., P. A. del Giorgio, and Y. T. Prairie. 2018. No longer a paradox: The interaction between physical transport and biological processes explains the spatial

distribution of surface water methane within and across lakes. Ecosystems **21**: 1073–1087. doi:10.1007/s10021-017-0205-1DO

Donis, D., S. Flury, A. Stöckli, J. E. Spangenberg, D. Vachon, and D. F. McGinnis. 2017. Full-scale evaluation of methane production under oxic conditions in a mesotrophic lake. Nat. Commun. **8**: 1661. doi:10.1038/s41467-017-01648-4DO

Duan, H., R. Ma, X. Xu, F. Kong, S. Zhang, W. Kong, J. Hao, and L. Shang. 2009. Two-decade reconstruction of algal blooms in China's Lake Taihu. Environ. Sci. Technol. **43**: 3522–3528. doi:10.1021/es8031852

Dyhrman, S. T., P. D. Chappell, S. T. Haley, J. W. Moffett, E. D. Orchard, J. B. Waterbury, and E. A. Webb. 2006. Phosphonate utilization by the globally important marine diazotroph *Trichodesmium*. Nature **439**: 68–71. doi:10.1038/nature04203DO

Fernandez, J. E., F. Peeters, and H. Hofmann. 2016. On the methane paradox: Transport from shallow water zones rather than in situ methanogenesis is the major source of CH_4 in the open surface water of lakes. J. Geophys. Res. Biogeosci. **121**: 2717–2726. doi:10.1002/2016JG003586

Ferry, J. G., and K. A. Kastead. 2007. Methanogenesis, p. 288–314. *In* R. Cavicchioli [ed.], Archae: Molecular and cellular biology. ASM Press.

Ghyczy, M., C. Torday, J. Kaszaki, A. Szabó, M. Czóbel, and M. Boros. 2008. Hypoxia-induced generation of methane in mitochondria and eukaryotic cells - an alternative approach to methanogenesis. Cell Physiol. Biochem. **21**: 251–258. doi:10.1159/000113766

Grossart, H.-P., K. Frindte, C. Dziallas, W. Eckert, and K. W. Tang. 2011. Microbial methane production in oxygenated water column of an oligotrophic lake. Proc. Natl. Acad. Sci. USA **108**: 19657–19661. doi:10.1073/pnas.1110716108

Guildford, S. J., H. A. Bootsma, E. J. Fee, R. E. Hecky, and G. Patterson. 2000. Phytoplankton nutrient status and mean water column irradiance in Lakes Malawi and Superior. Aquat. Ecosyst. Health Manag. **3**: 35–45. doi:10.1080/14634980008656989

Günthel, M., D. Donis, G. Kirillin, D. Ionescu, M. Bizic, D. F. McGinnis, H.-P. Grossart, and K. W. Tang. 2019. Contribution of oxic methane production to surface methane emission in lakes and its global importance. Nat. Commun. **10**: 5497. doi:10.1038/s41467-019-13320-0

Hampton, S., L. R. Izmest'eva, M. V. Morre, S. L. Katz, B. Dennis, and E. A. Silow. 2008. Sixty years of environmental change in the world's largest freshwater lake – Lake Baikal, Siberia. Glob. Chang. Biol. **14**: 1947–1958. doi:10.1111/j.1365-2486.2008.01616.x

Hartmann, J. F., M. Günthel, T. Klintzsch, G. Kirillin, H.-P. Grossart, F. Keppler, and M. Isenbeck-Schröter. 2020. High spatiotemporal dynamics of methane production and emission in oxic surface water. Environ. Sci. Technol. **54**: 1451–1463. doi:10.1021/acs.est.9b03182

Hemschemeier, A., and T. Happe. 2011. Alternative photosynthetic electron transport pathways during anaerobiosis in the green alga *Chlamydomonas reinhardtii*. Biochim. Biophys. Acta **1807**: 919–926. doi:10.1016/j.bbabio.2011.02.010

Ho, J. C., A. M. Michalak, and N. Pahlevan. 2019. Widespread global increase in intense lake phytoplankton blooms since the 1980s. Nature **574**: 667–670. doi:10.1038/s41586-019-1648-7

IPCC. 2013. Climate Change 2013: The physical science basis. Contribution of working group I to the fifth assessment report of the Intergovernmental Panel on Climate Change. Cambridge Univ. Press.

Juutinen, S., M. Rantakari, P. Kortelainen, J. T. Huttunen, T. Larmola, J. Alm, J. Silvola, and P. J. Martikainen. 2009. Methane dynamics in different boreal lake types. Biogeosciences **6**: 209–223. doi:10.5194/bg-6-209-2009

Kana, T. M., J. C. Cornwell, and L. Zhong. 2006. Determination of denitrification in the Chesapeake Bay from measurements of N_2 accumulation in bottom water. Estuaries Coast. **29**: 222–231.

Karl, D. M., L. Beversdorf, K. M. Björkman, M. J. Church, A. Martinez, and E. F. Delong. 2008. Aerobic production of methane in the sea. Nat. Geosci. **1**: 473–478. doi:10.1038/ngeo234

Keppler, F., J. T. G. Hamilton, M. Braß, and T. Röckmann. 2006. Methane emissions from terrestrial plants under aerobic conditions. Nature **439**: 187–191. doi:10.1038/nature04420DO

Khatun, S., and others. 2019. Aerobic methane production by planktonic microbes in lakes. Sci. Total Environ. **696**: 133916. doi:10.1016/j.scitotenv.2019.133916

Kirschke, S., and others. 2013. Three decades of global methane sources and sinks. Nat. Geosci. **6**: 813–823. doi:10.1038/ngeo1955

Klintzsch, T., G. Langer, G. Nehrke, A. Wieland, K. Lenhart, and F. Keppler. 2019. Methane production by three widespread marine phytoplankton species: Release rates, precursor compounds, and relevance for the environment. Biogeosciences. **16**: 4129–4144. doi:10.5194/bg-16-4129-2019-245

Kutovaya, O. A., R. M. L. McKay, and G. S. Bullerjahn. 2013. Detection and expression of genes for phosphorus metabolism in picocyanobacteria from the Laurentian Great Lakes. J. Great Lakes Res. **39**: 612–621. doi:10.1016/j.jglr.2013.09.009

Lecher, A. L., P.-C. Chuang, M. Singleton, and A. Paytan. 2017. Sources of methane to an Arctic lake in Alaska: An isotope investigation. J. Geophys. Res. Biogeosci. **122**: 753–766. doi:10.1002/2016JG003491

Lenhart, K., and others. 2012. Evidence for methane production by saprotrophic fungi. Nat. Commun. **3**: 1046. doi:10.1038/ncomms2049

Lenhart, K., T. Klintzsch, G. Langer, G. Nehrke, M. Bunge, S. Schnell, and F. Keppler. 2016. Evidence for methane production by the marine algae *Emiliania huxleyi*. Biogeosciences **13**: 3163–3174. doi:10.5194/bg-13-3163-2016

Li, L., B. Xue, S. Yao, Y. Tao, and R. Yan. 2018. Spatial–temporal patterns of methane dynamics in Lake Taihu. Hydrobiologia **822**: 143–156. doi:10.1007/s10750-018-3670-4

Lyu, Z., and Y. Liu. 2019. Diversity and taxonomy of methanogens, p. 1–22. *In* J. M. Alfons and D. Sousa [eds.], Biogenesis of hydrocarbons. Springer.

Murase, J., and A. Sugimoto. 2005. Inhibitory effect of light on methane oxidation in the pelagic water column of a mesotrophic lake (Lake Biwa, Japan). Limnol. Oceanogr. **50**: 1339–1343. doi:10.4319/lo.2005.50.4.1339

Peeters, F., J. E. Fernandez, and H. Hofmann. 2019. Sediment fluxes rather than oxic methanogenesis explain diffusive CH_4 emissions from lakes and reservoirs. Sci. Rep. **9**: 243. doi:10.1038/s41598-018-36530-w

Powell, R. J. 1972. Solubility of 16 gases in heptacosafluorotributylamine and carbon disulfide. J. Chem. Eng. Data **17**: 302–304. doi:10.1021/je60054a024

R Core Team. 2016. R: A language and environment for statistical computing. R Foundation for Statistical Computing. Accessed on Dec 2016. Available from https://www.R-project.org/

Repeta, D. J., S. Ferrón, O. A. Sosa, C. G. Johnson, L. D. Repeta, M. Acker, E. F. DeLong, and D. M. Karl. 2016. Marine methane paradox explained by bacterial degradation of dissolved organic matter. Nat. Geosci. **9**: 884–887. doi:10.1038/ngeo2837

RStudio Team. 2016. RStudio: Integrated development for R. RStudio, Inc. Available from http://www.rstudio.com/

Saunois, M., and others. 2016. The global methane budget 2000-2012. Earth Syst. Sci. Data **8**: 697–751. doi:10.5194/essd-8-697-2016

Signal Developers. 2013. signal: Signal processing. Accessed on June 2017. Available from http://r-forge.r-project.org/projects/signal/

Tang, K. W., D. F. McGinnis, K. Frindte, V. Brüchert, and H.-P. Grossart. 2014. Paradox reconsidered: Methane oversaturation in well-oxygenated lake waters. Limnol. Oceanogr. **59**: 275–284. doi:10.4319/lo.2014.59.1.0275

Tang, W. K., D. F. McGinnis, D. Ionescu, and H.-P. Grossart. 2016. Methane production in oxic lake waters potentially increases aquatic methane flux to air. Environ. Sci. Technol. Lett. **3**: 227–233. doi:10.1021/acs.estlett.6b00150

Thauer, R. K. 1998. Biochemistry of methanogenesis: A tribute to Marjory Stephenson: 1998 Marjory Stephenson Prize lecture. Microbiology **144**: 2377–2406. doi:10.1099/00221287-144-9-2377

Wang, Q., J. E. Dore, and T. R. McDermott. 2017. Methylphosphonate metabolism by *Pseudomonas* sp. populations contributes to the methane oversaturation paradox in an oxic freshwater lake. Environ. Microbiol. **19**: 2366–2378. doi:10.1111/1462-2920.13747

Whiticar, M. J. 1999. Carbon and hydrogen isotope systematics of bacterial formation and oxidation of methane. Chem. Geol. **161**: 291–314. doi:10.1016/S0009-2541(99)00092-3

Yao, M., C. Henny, and J. A. Maresca. 2016. Freshwater bacteria release methane as a by-product of phosphorus acquisition. Appl. Environ. Microbiol. **82**: 6994–7003. doi:10.1128/AEM.02399-16

Zheng, Y., and others. 2018. A pathway for biological methane production using bacterial iron-only nitrogenase. Nat. Microbiol. **3**: 281–286. doi:10.1038/s41564-017-0091-5

Acknowledgments

Peter Casper at the Leibnitz Institute of Freshwater Ecology and Inland Fisheries (IGB) is acknowledged for giving access to a GC/FID unit and flux chamber. We thank Uta Mallok (IGB) for providing nutrient data. Further thanks to Elke Mach (IGB), Armin Penske (IGB), and Michael Sachtleben (IGB) for technical support. Anke Penzlin from the German Environment Agency (Umweltbundesamt) kindly provided weather data. Funding was provided by the German Research Foundation (GR1540/21-1, 23-1, 28-1), the German Ministry of Education and Science (BMBF 01LC1501G), and European Commission/Horizon program (H2020 project ERA-PLANET). Open access funding enabled and organized by Projekt DEAL.

Conflict of Interest

None declared.

Submitted 30 May 2019
Revised 15 December 2019
Accepted 17 June 2020

Associate editor: Maria Maldonado